Using An Expanded Morris-Lecar Model to Determine Neuronal Dynamics In the Event of Traumatic Brain Injury

Ryan W. Tam
rwtam@ucsd.edu

Department of Bioengineering
University of California San Diego
La Jolla, CA 92093

Abstract

In the event of a traumatic brain injury, three primary physiological outcomes occur: the neurons become inactive at first, but through a process known as homeostatic synaptic plasticity (HSP), TNF-alpha is released from glial cells. This affects the excitatory and inhibitory neurotransmitter balance, which can lead to pro-epileptic effects. The nerve cells are also damaged, causing sodium and potassium channels to become chronically leaky, although ion pumps will respond. Finally, the cortex stimulates a current that yields a smaller frequency in the event of trauma. An extended Morris-Lecar model is used to model the dynamics of a single neuron, coupled PY-PY and PY-IN neurons, and a six neuron network in the event of these effects. The model incorporates features such as neurotransmitter-dependent synaptic currents, ion pump currents, and an excitatory cortical trauma current, which are varied to alter the injured neurons' firing of action potentials. Different trauma volumes and trauma types, such as focal and diffuse, are simulated in the six-neuron network. HSP mechanics, which adjust the neurotransmitter conductivities, are also examined within coupled neurons. Expectations are that with higher pump currents, deafferentation conductivities and trauma volumes, the amplitude of individual spikes are higher, but smaller peaks of bursts also exist, so the spiking rate is less. In the six-neuron network testing, focal trauma yields greater deafferentation effects than diffuse trauma. With HSP, the expectations are that IN reduces the firing rate so it requires a greater conductivity adjustment than with PY neurons.

1. Introduction

1.1 Background Neuroscience and Physiological Relevance

1.1.1 Release of TNF-alpha, and its effects on neurotransmitters

Trauma leads to chronic neural inactivity, causing an action potential to travel down the axon and terminate at synaptic terminals. The channels are depolarized to release calcium, causing astrocyte glial cells to release TNF-alpha, which are cell signaling proteins that can

induce inflammation. This whole process of releasing TNF-alpha in the face of neuronal inactivity is known as homeostatic synaptic plasticity, or HSP. This mechanism works to restore a stable activity pattern when the neural network is perturbed. However, overexpression of TNF-alpha as it binds to neurotransmitter-containing vesicles leads to insertion of excitatory AMPA and NMDA neurotransmitter receptors, and endocytosis of inhibitory GABA receptors. This shifts the balance to excitation through the insertion of AMPA, which can increase excitability in an uncontrollable manner and lead to paroxysmal activity and pro-epileptic effects.

1.1.2 Leaky Channels and Ion Pump Effects

Trauma damages nerve cells and renders membranes overly fluid, so many of the sodium channels become chronically leaky as they stay open for too long. This causes the pumps to respond. This continual pump and leak interplay triggers the sort of bizarre intermittent action potential bursts of injured neurons. The pump current consists of dynamic internal sodium and external potassium concentrations. Those concentrations further depend on the surface area of the nodal membrane, as well as the intracellular and extracellular volumes of the Node of Ranvier, so the surface geometry is accounted for.

1.1.3 Cortical Deafferentation

The neuron receives an excitatory current from the rest of the cortex. Typically, this conductance is stimulated randomly at a baseline Poisson rate of 50 Hz, but under trauma, the frequency can be reduced significantly from this value.

1.2 Goals

The goals are delineated in Figure 1, testing the consequences of trauma on four sets of neurons: single neurons, coupled pyramidal-pyramidal and pyramidal-inhibitory neurons, and neuronal network of six neurons. The coupled neurons and neuronal networks utilize three neurotransmitters: excitatory AMPA and NMDA, and inhibitory GABA. Several simulations are done testing the effects of these neurotransmitter conductivities, as well as modifying these conductivities based on firing rate to test for HSP. Simulations are also done adjusting for cortical deafferentation conductivities, as well as adjusting the sodium leak and pump currents.

2. Morris-Lecar Models

The complete model is described by the following equation:

$$C_m \frac{dV_m}{dt} = I_{ext} - I_{Na} - I_K - I_{leak} - I_{ad} - I_{syn} + I_{aff} - I_{Na\ leak} - I_{K\ leak} + I_{pump}$$

The full equations are found in the appendix. Analysis is done within a 200 millisecond time frame. For the purposes of this project, the following simplifications are made: 1) the axon injury is homogeneous even though it is spatially non-homogeneous. 2) For synaptic transmission within a neural network, the synapses are modeled as an ionic channel via Ohm's Law.

3. Results

3.1 Morris-Lecar, Pump and Cortical Deafferentation Models

A $$C_m \frac{dV_m}{dt} = I_{ext} - I_{Na} - I_K - I_{Na\,leak} - I_{K\,leak} + I_{pump}$$

B $$C_m \frac{dV_m}{dt} = I_{ext} - I_{Na} - I_K - I_{leak} - I_{ad} + I_{aff}$$

The pumps combat the trauma-induced leaky channels, as expressed in equation A. As seen in figure 2A, two pump currents, 30 $\frac{\mu A}{cm^2}$ and 170 $\frac{\mu A}{cm^2}$, were used. At lower maximum pump currents, tonic low amplitude "slow" oscillations occur, with shorter interburst intervals, and these pathological excitability patterns are characteristic of several forms of traumatic injury. At higher maximum pump currents, there is repetitive action potential activity characterized by higher spiking amplitude, although firing rate decreases due to longer burst intervals, as expressed in Figure 2B. These intervals are longer because the sodium/potassium pump better mediates the restoration of the ion gradients, which is why the high amplitude spikes are separated by low amplitude oscillations.

In describing the pump mechanics for the pump current, there is an increase in $[Na+]_i$ and $[K+]_o$ to yield the first spike, and then oscillations of $[Na+]_i$ and $[K+]_o$ between concentrations for the duration. This is what is known as a stable limit cycle, because as time goes to infinite, the voltage excursion is between -20 and 10 mV, so the same spiking patterns are generated continuously. The pump mechanics for a 170 $\frac{\mu A}{cm^2}$ current are similar, but there is a higher voltage excursion and less of a firing rate, so the limit cycle is less dense in Figure 2D.

Cortical trauma is accounted for through an injection of an excitatory current, as expressed in equation B. In the intact, zero trauma model, Volman's group [2] saw spiking rates of around 50 Hz, or 50 $\frac{spikes}{second}$. In Figure 2E, zero deafferentation yields 10 spikes, so within the 200 ms timeframe, this means there are 50 $\frac{spikes}{second}$, matching Volman's rate. However, as seen in Figures 2E-2H, with greater deafferentation, the spiking amplitude is higher, but since many smaller peaks which are unable to hit threshold, the spiking rate is less. This significant reduction of spontaneous firing leading to slow oscillations was detected in deep cortical layers by Avramescu's group[6] after they undercut and deafferentated a suprasylvian gyrus, as seen in Figure 2I. Low trauma sees up to 35% degradation of spiking rate from the intact model, intermediate sees from 35-65%, and high trauma sees above 65% degradation. The six neuron network tests cases of each of these forms of trauma, based on the deafferentation conductance adjustments.

3.2 Morris-Lecar, Coupled Neurons with Excitatory AMPA-NMDA and Inhibitory AMPA-GABA Neurotransmitters, and HSP Testing

A
$$C_m \frac{dV_m}{dt} = I_{ext} - I_{Na} - I_K - I_{leak} - I_{ad} - I_{syn,AMPA}$$
$$C_m \frac{dV_m}{dt} = I_{ext} - I_{Na} - I_K - I_{leak} - I_{ad} - I_{syn,NMDA}$$

B
$$C_m \frac{dV_m}{dt} = I_{ext} - I_{Na} - I_K - I_{leak} - I_{ad} - I_{syn,AMPA}$$
$$C_m \frac{dV_m}{dt} = I_{ext} - I_{Na} - I_K - I_{leak} - I_{ad} - I_{syn,GABA}$$

For PY-PY neurons with AMPA-NMDA neurotransmitters characterized by equations A, with increased AMPA conductivities, there are smaller interburst intervals. However, most of them form sub-threshold oscillations (STOs) which do not form action potentials, so the spike rate is reduced. Increased NMDA conductivities do not affect the interburst interval but it

increases the amplitude of the second neuron's spike. With both conductivities increased there is a "coupling" effect in that both neurons adapt to the same spike patterns, taking characteristics of both neurotransmitter effects. Thus, while there are smaller bursts that characterize AMPA, but there would be fewer of them due to the effects of NMDA, leading to a smaller spike rate as seen in Figure 3E. For PY-IN neurons with AMPA-GABA neurotransmitters seen in equations B, higher AMPA and GABA conductivities yield greater spiking amplitude for the first and second neurons, respectively, but GABA also generates larger interburst intervals. When both conductivities increase together, both neurotransmitter properties are accounted for, and GABA's inhibitory properties yield a significantly smaller spike rate, with a minimum of 5 spikes for PY-IN neurons as opposed to 8 spikes for PY-PY neurons, when comparing Figures 3E and 3K.

Another aspect to explore is the post-traumatic homeostatic synaptic plasticity, which adjusts the synaptic conductivity of the coupled neurons, $g_{PY\text{-}PY}$ and $g_{PY\text{-}IN}$. This conductivity changes based on the differing firing rates as g_{AMPA}, g_s and g_{GABA} are varied. The preset target rate of pyramidal neuron firing is at 45 Hz, and a homeostatic update convergence constant is used to adjust the conductance. As seen in Figure 3F, for PY-PY neurons, there is slight upregulation of conductance for cases with greater g_s, and slight downregulation of conductance for cases with greater g_{AMPA}, of which the higher firing rate corresponds to upregulation and therefore release of TNF-alpha from glial cells. From Figure 3L, for PY-IN neurons, there is a sign change distinguishing it from PY-PY neurons, so a higher GABA conductivity leads to greater downregulation of synaptic conductance, while a higher AMPA conductivity leads to slight upregulation of conductance. For PY-PY neurons, the maximum extent of homeostatic adjustment from 0 to 2 $\frac{mS}{cm^2}$ for AMPA and NMDA conductivities is +6.7%, while for PY-IN neurons, it is -13.6% for AMPA and GABA conductivities. The rate is double for PY-IN neurons because GABA drastically reduces the spike train, and the adjustment is based on firing rate, so the magnitude of the adjustment is expected.

3.3 Morris-Lecar, Six Neuron Network, Testing Focal, Scaled Focal, and Cortical Trauma

Deafferentation testing is conducted on a network of six neurons, where after every four PY neurons, there is an IN neuron, an idea adapted by Volman[2]. As shown in Figure 4A, the network is characterized by feedforward inhibition, in which the inhibitory fifth neuron reduces the spiking amplitude and thus excitation of the sixth neuron. A feedback loop re-transmits the weakened signal from the sixth neuron back to the first, with GABA's inhibitory effects also reducing the spiking rate of all neurons. Three types of trauma are simulated: focal trauma, in Figure 4B, is characterized by a spatially contiguous subpopulation of neurons which are deafferentated, and diffuse trauma, in Figure 4C, has a random selection of neurons which are deafferented. These simulations only vary the trauma volume, or the fraction of neurons that are deafferentated, while keeping the neurotransmitter conductivities, deafferentation conductivities and maximum pump current constant, at 2 mS, 0.5 $\frac{mS}{cm^2}$, and 170$\frac{\mu A}{cm^2}$, respectively. However, the third simulation for scaled focal trauma varies both trauma volume and cortical deafferentation

conductivities. This is a more realistic model as deafferentation, which is adjusted from low to high as seen in Figure 4G, increases for closer neurons and decreases in scale for those farther away.

In comparing the simulations for focal and diffuse trauma, it is clear that which neuron is deafferentated affects the spike rate, even with the same trauma volume. For example, at 50% trauma for both cases, which compares Figure 5B with 5G, a deafferented inhibitory neuron yields a smaller minimum spiking rate when comparing Figures 5D and 5H. Also, under the same trauma volume, diffuse trauma has less deafferentation effects than focal trauma, because the excitatory neurons have higher spiking rates in diffuse trauma when comparing Figures 5A-C with 5E-G. In simulating scaled focal trauma, lower cortical deafferentation conductivities, as seen in simulations 2, 3 and 4 in Figure 4F, have higher spiking rates, and this is reflected in Figure 5I. However, larger conductivities decrease the spike rate, as seen in Figure 5K.

3.4 Morris-Lecar, Six Neuron Network: Combining the Deafferentation Current, Pumps and Neurotransmitter Effects

Figure 6 combines all the elements discussed and tests for varying neurotransmitter conductivities, deafferentation conductivities, and maximum pump currents, and these changes are the same across all six neurons. The trend holds as before: as all the test values increase, particularly GABA conductivities, the spiking amplitude gets progressively higher but the interburst interval gets larger, so the spike rate is significantly less.

4. Conclusion

The models in this paper were able to recreate a scenario of a traumatic brain injury, by implementing the effects of cortical deafferentation, ion leaks, ion pumps, and neurotransmitters on single neurons, coupled neurons and a six-neuron network. In addition, several simulations were conducted to elucidate the effects of HSP on PY-PY and PY-IN neurons. The six neuron network confirmed the spiking patterns that were seen in individual and coupled neurons. With the exception of the pumping mechanism, this model is not dynamic, and it only tests coupled neurons. For future research, differential equations will be set up to evolve the cortical deafferentation and synaptic conductance values. Also, a cortical neural network of 20 by 20 neurons will be set up, 80% of which are PY-PY neurons and the remaining 20% are PY-IN neurons. Data acquired from a dynamic, larger-scale model will therefore be more accurate.

Acknowledgments

I wish to thank Gert Cauwenberghs, Jeffrey Bush, and TAs Chul Kim and Bruno Pedroni for educating me in the topic of neurodynamics so those concepts could be reflected in this project.

References

[1] Yu, Na, et al. "Spontaneous excitation patterns computed for axons with injury-like impairments of sodium channels and Na/K pumps." *PLoS Computational Biology* 8.9 (2012): e1002664.
[2] Volman, Vladislav, Maxim Bazhenov, and Terrence J. Sejnowski. "Divide and Conquer: Functional Segregation of Synaptic Inputs by Astrocytic Microdomains Could Alleviate Paroxysmal Activity Following Brain Trauma."*PLoS computational biology* 9.1 (2013): e1002856.
[3] Rudolph, Michael, et al. "A method to estimate synaptic conductances from membrane potential fluctuations." *Journal of neurophysiology* 91.6 (2004): 2884-2896.
[4] Timofeev, Igor, et al. "Age dependency of trauma-induced neocortical epileptogenesis." *Frontiers in cellular neuroscience* 7 (2013).
[5] Volman, Vladislav, and Laurel J. Ng. "Computer Modeling of Mild Axonal Injury: Implications for Axonal Signal Transmission." (2013).
[6] Avramescu, Sinziana, Dragos A. Nita, and Igor Timofeev. "12 Posttraumatic reactive gliosis is associated with paroxysmal activity and impaired potassium clearance." *Résumé* 12: 12-3.
[7] Nita, Dragos A., et al. "Waking–Sleep Modulation of Paroxysmal Activities Induced by Partial Cortical Deafferentation." *Cerebral Cortex* 17.2 (2007): 272-283.

Appendix

SET OF EQUATIONS USED:

Current (μA)	Name	Equation	Description/Notes
I_{ext}	External Injected Current	$40 + floor\ (\frac{t}{20})$	Initial injected current is 40 μA and after every 20 ms the current increases by 1 μA
I_{Na}	Sodium Channel Current	$G_{Na} m_{\infty} (V_m - E_{Na})$	Current is based on kinetics m_{∞} which is voltage dependent
I_K	Potassium Channel Current	$G_K \dot{\omega} (V_m - E_K)$	Current is based on kinetics $\dot{\omega}$ which evolves based on a differential equation
I_{leak}	Leak current	$G_L (V_m - E_L)$	
I_{ad}	Spike adaptation current	$G_a z (V_m - E_K)$	
$I_{syn,AMPA}$	Synaptic current for AMPA	$G_{syn,AMPA} r_{AMPA} (V_{post} - E_{AMPA})$	For PY-PY synapses. $G_{syn,AMPA}$ is varied via simulation testing, while r_{AMPA} evolves from a differential equation dependent on concentration
$I_{syn,NMDA}$	Synaptic current for NMDA	$\frac{g_s - g_f}{1 + 0.264 \times e^{-0.06 \times V_m}} r_{NMDA} (V_{post} - E_{NMDA})$	For PY-PY synapses. g_s or NMDA slow conductivity is varied via simulation testing while g_f is constant
$I_{syn,GABA}$	Synaptic current for GABA	$G_{syn,GABA} r_{GABA} (V_{post} - E_{GABA})$	For PY-PY synapses. $G_{syn,GABA}$ is varied via

			simulation testing, while r_{GABA} evolves from a differential equation dependent on concentration
I_{aff}	Deafferentation Current for Cortical Trauma	$G_{ex}(V_m - E_{ex})$	G_{ex} is varied via simulation testing.
$I_{Na\ leak}$	Sodium leak current	$G_{Na\ leak}(V_m - E_{NaNernst})$	Based on Nernst reversal potentials for sodium.
$I_{K\ leak}$	Potassium leak current	$G_{K\ leak}(V_m - E_{KNernst})$	Based on Nernst reversal potentials for potassium.
I_{pump}	Pump current	$I_{maxpump}(1 + \frac{K_{M_K}}{[K+]_o})^{-2} \times (1 + \frac{K_{M_{Na}}}{[Na+]_i})^{-3}$	Based on Michaelis Menten dissociation constants, and $[K+]_o$ and $[Na+]_i$ evolve through differential equations based on ion pump and leak currents as well as nodal membrane area and volume.
$I_{Na\ pump}$	Sodium ion pump current	$3 \times I_{pump}$	Exchanges three $[Na+]_i$ ions…
$I_{K\ pump}$	Potassium ion pump current	$-2 \times I_{pump}$	…for two $[K+]_o$ ions

Other Values	**Name**	**Units**	**Equation**
m_∞	Receptor channel kinetics, Na	1	$0.5 \times (1 + \tanh(\frac{V_m+1.2}{23}))$
$\acute{\omega}_\infty$	Receptor Channel kinetics, K	1	$0.5 \times (1 + \tanh(\frac{V_m+2}{21}))$
$E_{NaNernst}$	Nernst equation for Sodium	mV	$-V_t \times log\frac{[Na]_{int}}{[Na]_{ext}}$
$E_{KNernst}$	Nernst equation for Potassium	mV	$-V_t \times log\frac{[K]_{int}}{[K]_{ext}}$
$[conc]$	Concentration of particular neurotransmitter in synaptic cleft	mM	$\frac{[conc]_{max}}{(1 + e^{\frac{-(V_{pre}-V_p)}{k_p}})}$
g_{PY-PY}	Post-traumatic HSP, PY-PY synaptic conductivity	mS	$g_{PY-PY} + \alpha_{HSP}(v_0 - v_{firing\ rate})$
g_{PY-IN}	Post-traumatic HSP, PY-IN synaptic conductivity	mS	$g_{PY-IN} - 0.5 \times \alpha_{HSP}(v_0 - v_{firing\ rate})$
HSP	Maximum of HSP change, for PY-PY neurons	1	$100 \times \frac{(g_{PY-PY}(\max G_{syn,AMPA}, \max G_s) - g_{PY-PY}(\min G_{syn,AMPA}, \min G_s))}{g_{PY-PY}(\min G_{syn,AMPA}, \min G_s)}$

HSP	Maximum of HSP change, for PY-IN neurons	1	$100 \times \frac{(g_{PY-PY}(\max G_{AMPA}, \max G_{GABA}) - g_{PY-PY}(\min G_{AMPA}, \min G_{GABA}))}{g_{PY-PY}(\min G_{AMPA}, \min G_{GABA})}$

Differential Equations, other than $\frac{dV_m}{dt}$	**Name**	**Equation**
$\frac{d\acute{\omega}}{dt}$	Change in K receptor channel kinetics	$0.15 \times (\acute{\omega}_{\infty} - \acute{\omega}) \times \cosh(\frac{V_m + 2}{42})$
$\frac{dz}{dt}$	Change in spike adaptation channel kinetics	$(5 \times 10^{-3}) \times (\frac{1}{1 + e^{\frac{-V_m}{5}}} - z)$
$\frac{dr_{AMPA}}{dt}$	Change in AMPA channel kinetics	$\alpha_r \times [conc] \times (1 - r_{AMPA}) - \beta_r \times r_{AMPA}$
$\frac{dr_{GABA}}{dt}$	Change in GABA channel kinetics	$\alpha_r \times [conc] \times (1 - r_{GABA}) - \beta_r \times r_{GABA}$
$\frac{dr_{NMDA}}{dt}$	Change in NMDA channel kinetics	$\alpha_r \times [conc] \times (1 - r_{NMDA}) - \beta_r \times r_{NMDA}$
$\frac{d[K+]_o}{dt}$	Change in external potassium concentration	$-\frac{(I_K + I_{Kpump} + I_{Kleak})A}{FVol_{int}}$
$\frac{d[Na+]_i}{dt}$	Change in internal sodium concentration	$-\frac{(I_{Na} + I_{Napump} + I_{Naleak})A}{FVol_{int}}$

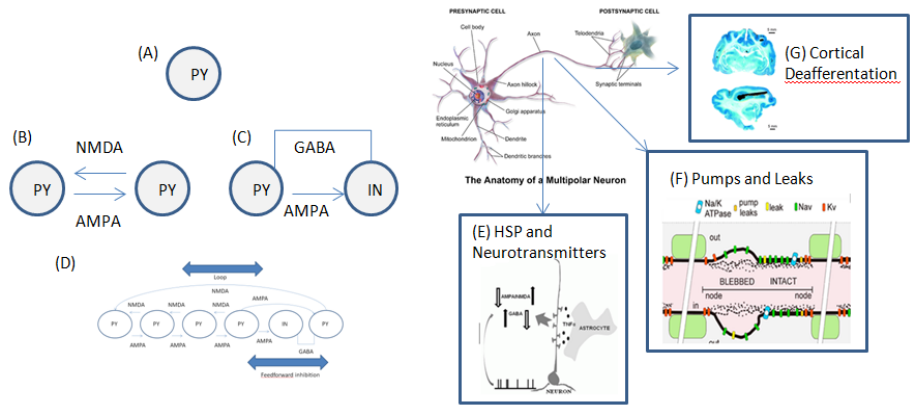

FIGURE 1: **Schematic illustrating the consequences of trauma as tested in this paper.** These consequences are initially tested on (A) single neurons, coupled (B) PY-PY and (C) PY-IN neurons, and (D) a 6-neuron network. The consequences include (E) Release of TNF-alpha, and its effects on neurotransmitter receptors. The balance is shifted towards excitation through homeostatic synaptic plasticity (HSP). (F) Leaky Channels and Ion Pump Effects. The traumatic mechanical insult injures the Node of Ranvier and "blebs" the bilayer. (G) Cortical Deafferentation Current, received from the rest of the cortex. Frontal and sagittal brain sections are stained to determine the amount of deafferentation in experiments.

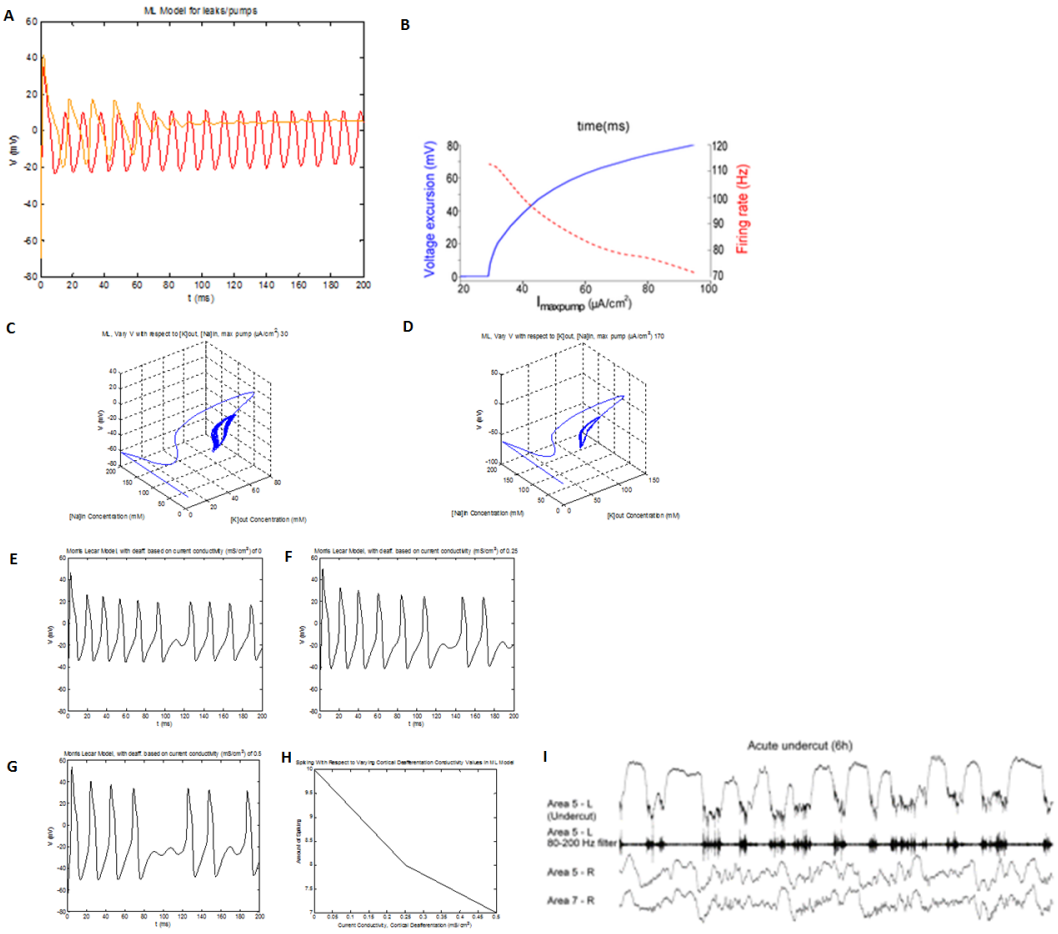

FIGURE 2: Single Neuron Tests With Respect to Pump Currents (A-D) and with respect to Cortical Deafferentation (E-I). (A-D) **Voltage spiking with respect to varying sodium and potassium reversal potentials, for different maximum pump currents**. At first, $[Na+]_i$ is 10 mM, while $[K+]_o$is 5 mM. (A) The spike train over a time frame of 200 ms, where 30 $\frac{\mu A}{cm^2}$ is shown in red and 170 $\frac{\mu A}{cm^2}$ is shown in orange. (B) Correlation between maximum current pump, voltage spiking amplitude and firing rate [1]. (C) Complete three-dimensional representation of voltage excursion for a pump current of 30 $\frac{\mu A}{cm^2}$, based on $[Na+]_i$ and $[K+]_o$. (D) Complete three-dimensional representation of voltage excursion for a pump current of 170 $\frac{\mu A}{cm^2}$, based on $[Na+]_i$ and $[K+]_o$. (E-I) **Cortical Deafferentation of a Single Morris-Lecar Neuron, Simulations. (**E), (F) and (G). Modeling cortical deafferentation of the single neuron, with varying current conductivities of 0, 0.25 and 0.5 $\frac{mS}{cm^2}$. (H). Spike rate goes down with greater cortical deafferentation, because the smaller peaks are unable to hit threshold, but the individual spikes are larger. (I) In experimentation, a knife enters the cortex of chronically implanted cats to perform the undercut, leading to an acutely partially deafferentated cortex. Stained frontal and sagittal brain sections were excised [7], and the left hemisphere denoted by L is deafferentated and characterized by a highly increased amplitude as compared to the right hemisphere, R. These experimental effects are verified in the simulations seen from A-D.

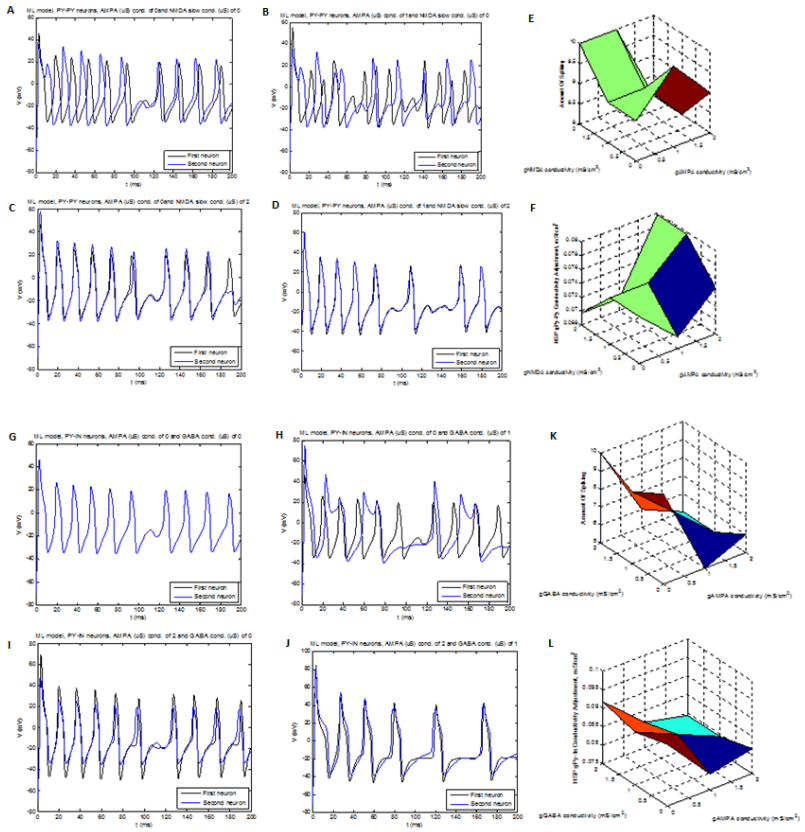

FIGURE 3. **Coupled Neuron Tests For PY-PY Neurons (A-F) and PY-IN Neurons (G-L) With Respect to Neurotransmitter Conductivities (A-D, G-J), Spike Rate (E, K) and HSP (F, L).** (A-D) **Varying conductivities of PY-PY Neuron.** (A): Coupled PY-PY Neuron with zero AMPA and NMDA conductivities. (B). Increasing AMPA conductivity while keeping NMDA conductivity at zero, characterized by shorter interburst intervals. (C). Increasing NMDA conductivity while keeping AMPA conductivity at zero. (D). The combination scenario where AMPA and NMDA conductivity are both increased, taking properties of both neurotransmitters. (E) Measuring Spike Rate. Actual spikes above threshold by varying the AMPA/NMDA neurotransmitter conductivity values. Above threshold is defined as a voltage value above 0 mV. gAMPA and gNMDA conductivities are varied from 0 to 2 $\frac{mS}{cm^2}$. (F) Measuring HSP. Conductivity adjustment of PY-PY Neurons via HSP, by varying the AMPA/NMDA neurotransmitter conductivity values. The initial value of the pyramidal-pyramidal neuron synaptic conductance is 0.074 $\frac{mS}{cm^2}$. (G-J). **Varying conductivities of PY-IN neuron**. (G) Coupled PY-IN Neuron with zero AMPA and GABA conductivities. (H) Increasing AMPA conductivity while keeping GABA conductivity at zero. (I) Increasing GABA conductivity while keeping AMPA conductivity at zero. (J) The combination scenario where AMPA and GABA conductivity are both increased, taking properties of both neurotransmitters. (K) Measuring Spike Rate. Above threshold is defined as a voltage value above 0 mV. gAMPA and gGABA conductivities are varied from 0 to 2$\frac{mS}{cm^2}$. (L) Measuring HSP. Conductivity adjustment of PY-IN Neurons via homeostatic synaptic plasticity, by varying the AMPA/GABA neurotransmitter conductivity values. The initial value of the pyramidal-inhibitory neuron synaptic conductance is 0.089 $\frac{mS}{cm^2}$.

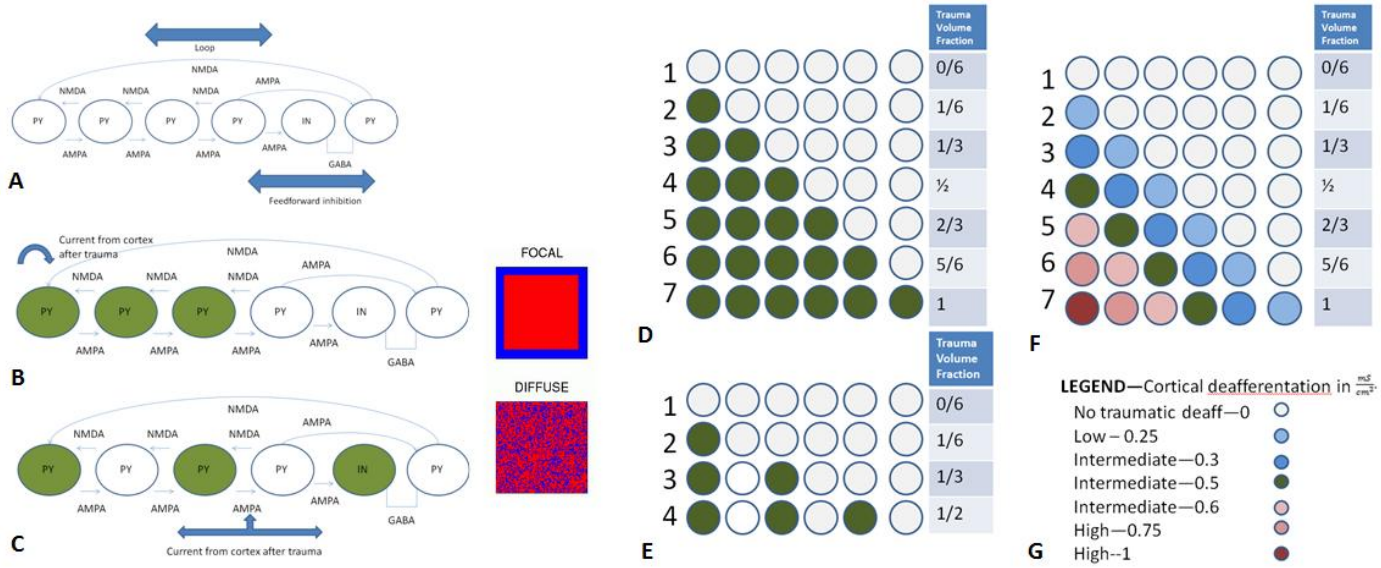

FIGURE 4: The Six by One Neuronal Network Test, schematics. (A-C) Neuronal architecture, and types of trauma tested on the network. (D-G) Simulation schematics, tested for the architecture. In A , B and C, only trauma volume is varied. Trauma volume is the fraction of neurons that are deafferented, or color-coded in the diagram, over the total amount of neurons (6 in this case). In F, cortical deafferentation values and trauma volume are varied. (A) Neuronal architecture for a six by one neuronal network. (B) An example model of focal trauma. (C) An example model of diffuse cortical trauma. (D) Simulations for focal trauma, for an intermediate trauma cortical deafferentation value of $0.5\,\frac{mS}{cm^2}$. Seven simulations are done, with an increasing trauma volume fraction. (E) Simulations for diffuse cortical trauma, for an intermediate trauma cortical deafferentation value of $0.5\,\frac{mS}{cm^2}$. Four simulations are done, with an increasing trauma volume fraction. (F) Simulations for focal trauma, for a for low, intermediate and high cortical deafferentation values that are varied increasingly by scale. (G) Legend illustrating the amount of traumatic deafferentation on color-coded neurons.

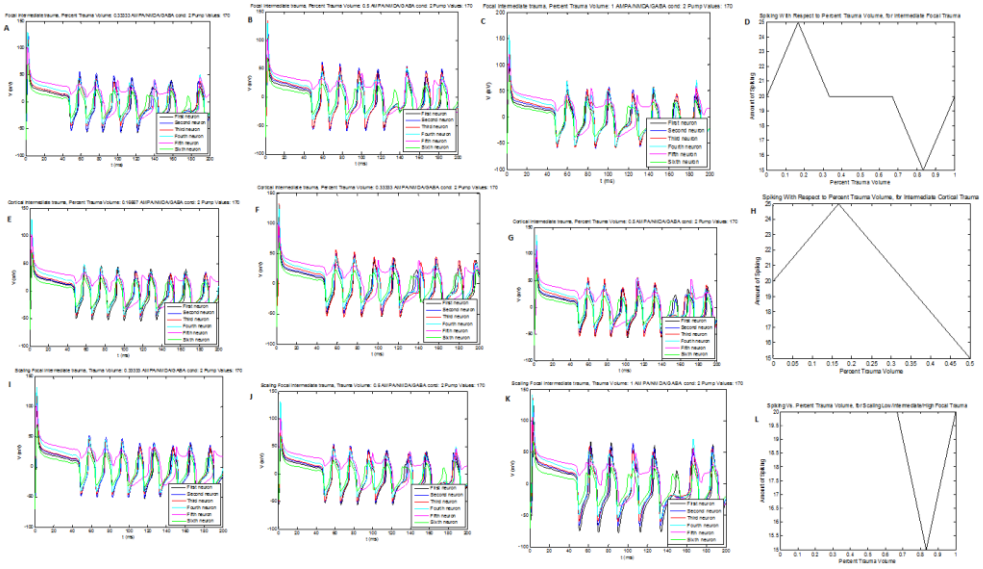

FIGURE 5: **The Six by One Neuronal Network Test**, **Simulations of Focal and Cortical Diffuse Trauma for Constant Cortical Deafferentation Values, and For Focal Trauma for Scaled Low to High Deafferentation Values.** The feedforward inhibition and subsequent loop back to the first neuron helps to keep the neurons at roughly the same level of minimum firing across trauma volumes. (A-D) Simulations of focal trauma, or Scenario D, in figure 4. Focal trauma volume of (A) 33.3%, (B) 50% and (C) 100%, and (D) the minimum amount of spiking for any of the six neurons relative to trauma volume. (E-H) Simulations of diffuse cortical trauma, or Scenario E, in figure 4. Diffuse trauma volume of (E) 16.7%, (F) 33.3% and (G) 50%, and (H) the minimum amount of spiking for any of the six neurons relative to trauma volume. (I-L): Simulations of Scenario F in figure 4. Simulations for focal trauma, for a for low, intermediate and high cortical deafferentation values that are varied increasingly by scale, (A) 33.3%, (B) 50% and (C) 100%. (D) The minimum amount of spiking for any of the six neurons relative to trauma volume.

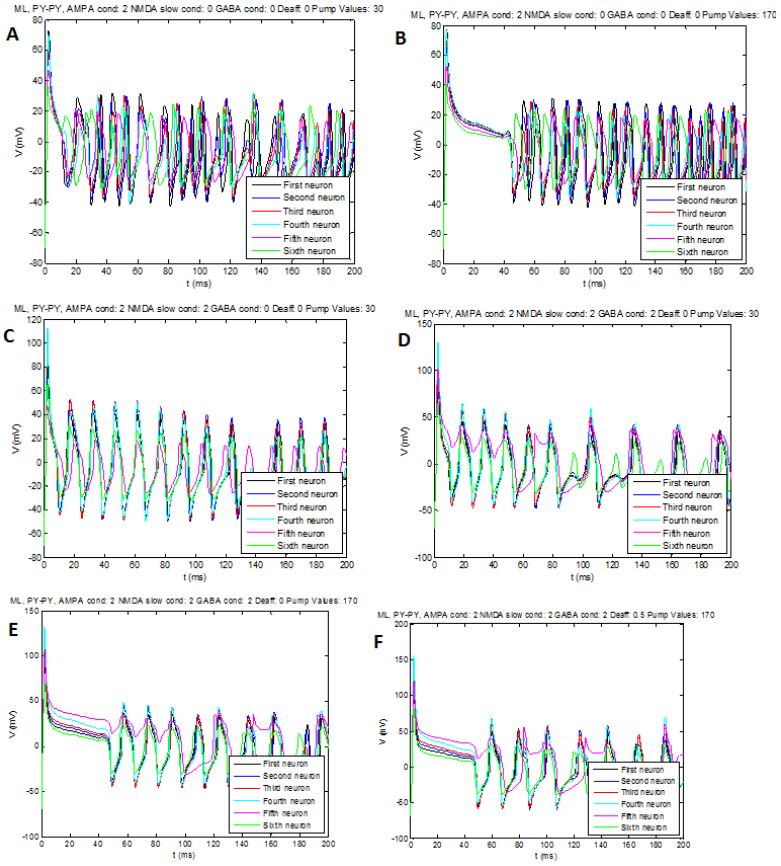

FIGURE 6: **The Six by One Neuronal Network Test**, **Simulations Varying Pump and Deafferentation Currents, and Neurotransmitter Conductivities.** (A) Baseline graph showing spiking with 2 mS AMPA conductivity and a pump current of $30\frac{\mu A}{cm^2}$. (B) Increased pump current relative to baseline. (C) Increased NMDA conductivity relative to baseline. (D) Increased NMDA and GABA conductivity relative to baseline. (E) Increased NMDA and GABA conductivities, and increased maximum pump current relative to baseline. (F) Increased NMDA and GABA conductivities, increased maximum pump current and increased deafferentation current relative to baseline.